

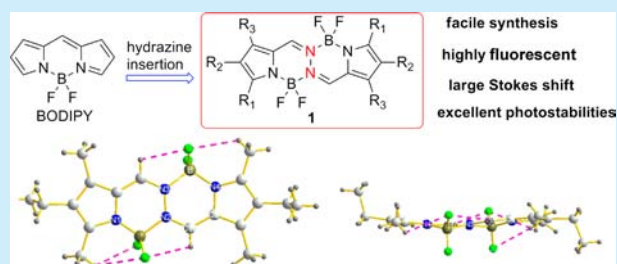
Highly Fluorescent  $\text{BF}_2$  Complexes of Hydrazine–Schiff Base Linked Bispyrrole

Changjiang Yu, Lijuan Jiao,\* Ping Zhang, Zeya Feng, Chi Cheng, Yun Wei, Xiaolong Mu, and Erhong Hao\*

Laboratory of Functional Molecular Solids, Ministry of Education, Anhui Laboratory of Molecule-Based Materials, School of Chemistry and Materials Science, Anhui Normal University, Wuhu, Anhui 241000, China

## Supporting Information

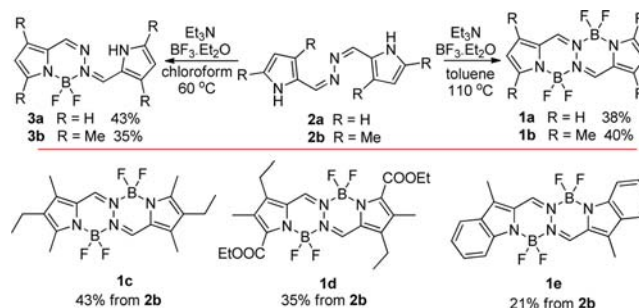
**ABSTRACT:** A series of  $\text{BF}_2$  complexes of hydrazine–Schiff base linked bispyrrole have been prepared from a simple two-step reaction from commercially available substances and are highly fluorescent in solution, film, and solid states with larger Stokes shift and excellent photostabilities comparable or even super to those of their BODIPY analogues. These resultant fluorescent dyes are highly susceptible to the postfunctionalization, as demonstrated in this work via the Knoevenagel condensation to introducing functionalities or tether groups to the chromophore.



Fluorescent dyes have attracted increasing research interest in highly diverse research fields, for example, as molecular probes in biomedical labeling and analysis and as organic electronics in material science.<sup>1</sup> Among those, BODIPY (4,4-difluoro-4-bora-3a,4a-diaza-*s*-indocene) derivatives as the well-known organoboron complexes have attracted wide research efforts with remarkable achievements due to their rich chemistry and their excellent photophysical properties.<sup>2,3</sup> Despite their intense fluorescence in solution, most BODIPYs have weak fluorescence in the solid state due to self-absorption closely associated with their narrow Stokes shift, which limits their further applications as optoelectronic devices. Many organoboron complexes,<sup>4–7</sup> such as the *N,N*  $\pi$ -conjugated boron(III) complexes ( $\text{B}-\text{D}^8$  in Figure 1), have been prepared as BODIPY analogues to overcome this problem.

Recently, we have prepared several hydrazine–Schiff base linked bispyrrole **2** (Scheme 1) from the simple condensation of commercially available 2-formylpyrrole with hydrazine in high yields. We rationalized that compound **2** would chelate with

## Scheme 1. Syntheses of Complexes 1a–e and 3a,b



boron(III) atom to form either the six-membered-ring  $\text{BF}_2$ -chelating complex **1** or the five-membered-ring chelating complex **A** (Figure 1). Among those, complex **1** as the hydrazine-inserted BODIPY would afford a larger Stokes shift while maintaining the easy postfunctionalization ability and the easily tunable photophysical properties of their BODIPY analogues. While this manuscript was in preparation, Ziegler's group reported the synthesis of two symmetrical pyrrole– $\text{BF}_2$  complexes.<sup>9</sup> Herein, we report the efficient synthesis, the characterizations, and the property studies of a series of  $\text{BF}_2$  complexes of hydrazine–Schiff base linked bispyrrole **1**, which are highly fluorescent in solution, film, and solid states via a simple two-step reaction from commercially available substances.

The  $\text{BF}_2$  complexation of compound **2a** with  $\text{BF}_3\cdot\text{OEt}_2$  in dichloromethane yields a mixture of two products according to TLC (a strong fluorescence one and a weak fluorescence one). The former was later confirmed to be the diborate complex **1a**, and the later was identified to be monoborate complex **3a** as

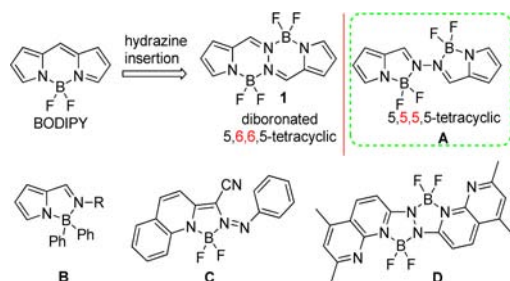


**Figure 1.** Chemical structures of BODIPY, the six-membered-ring  $\text{BF}_2$  chelating complex **1**, and the five-membered-ring  $\text{BF}_2$  chelating **A** and some representative literature-reported  $\pi$ -conjugated *N,N*-boron(III) complexes **B–D**.

Received: April 22, 2014

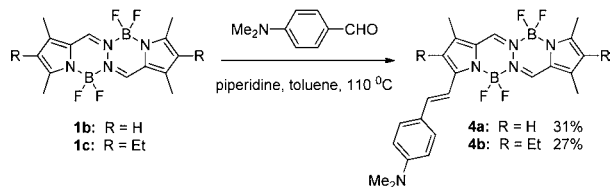
Published: May 21, 2014

confirmed by the X-ray diffraction results. Although several five-membered-ring chelating examples such as **B–D** (Figure 1) have been reported,<sup>8</sup> the variation of reaction conditions in our system could not afford any of the other expected five-membered-ring chelating product **A** or even its monoborate analogue.

By optimizing the reaction conditions, complex **1a** was generated exclusively in toluene at 110 °C, while the monoborate complex **3a** was mainly obtained in chloroform at 60 °C (Scheme 1). A similar reaction was observed for the BF<sub>2</sub> complexation of compound **2b** to give dyes **1b** and **3b** in 40% and 35% yields, respectively. To test the versatility of this reaction, hydrazine–Schiff bases **2c–e** were also prepared from the condensation of their corresponding 2-formylpyrrole derivatives and even their analogue 2-formyl(3-methyl-1*H*-indole) with hydrazine and were used for the subsequent BF<sub>2</sub> complexation in toluene at 110 °C, from which the desired complexes **1b–e** in 21–43% isolated yields (Scheme 1).

These resultant complexes **1** are susceptible to the postfunctionalization. For example, complexes **1b** and **1c** show reactivities comparable to those of their BODIPY analogues in Knoevenagel condensation reaction<sup>10</sup> with aromatic aldehyde, like 4-*N,N*-dimethylbenzaldehyde demonstrated in this work (Scheme 2), to introducing various functionalities or tether

#### Scheme 2. Postfunctionalization of **1b** and **1c** through Knoevenagel Condensation To Generate **4a** and **4b**



groups to the chromophore. All these resultant complexes were characterized by NMR and HRMS. Among those, complexes **1a**, **1b**, **1c**, **3a**, and **3b** were further characterized by X-ray crystallographic analysis (Figure 2).

The crystals suitable for X-ray analysis were obtained from the slow evaporation of the dichloromethane solutions of these complexes. There are four rigid planar ring structures in the chromophore of complexes **1a–c**: two five-membered pyrrole units at the periphery and two BF<sub>2</sub>-containing six-membered rings in the center, with only the fluorine atoms and the alkyl substituents (**1b** and **1c**) deviating from these plane chromophore. The dihedral angles of two pyrrole rings in the new formed chromophore are less than 2.7° (Table S1, Supporting Information), indicating the existence of an inversion center (*C*<sub>2h</sub> symmetry) in complexes **1a–c**. Similarly, the formation of one six-membered-ring BF<sub>2</sub>-chelating structure was also observed in the monoborate complexes **3a** and **3b**. The bond lengths in the pyrrolic units of these complexes **1a–c** and **3a,b** are similar to those observed in BODIPY derivatives,<sup>11</sup> indicating the remaining of the aromaticity of the peripheral pyrrole units at the edge.

Intramolecular C–H···F hydrogen bonds between F atoms and various hydrogen atoms (*C*<sub>a</sub> and *C*<sub>m</sub> in Table S1, Supporting Information) are formed due to the strong electron negativity of the F atom.<sup>11a</sup> The *C*<sub>m</sub>–F distances range from 2.88 to 3.09 Å, while the *C*<sub>a</sub>–F distances are significantly longer (3.10–3.52 Å). In the <sup>1</sup>H NMR spectra, the chemical shifts for hydrogen atoms at *C*<sub>a</sub> are both at around 2.50 ppm for **1b** and the corresponding 1,3,5,7-tetramethylBODIPY,<sup>11b</sup> while the chemical shifts for

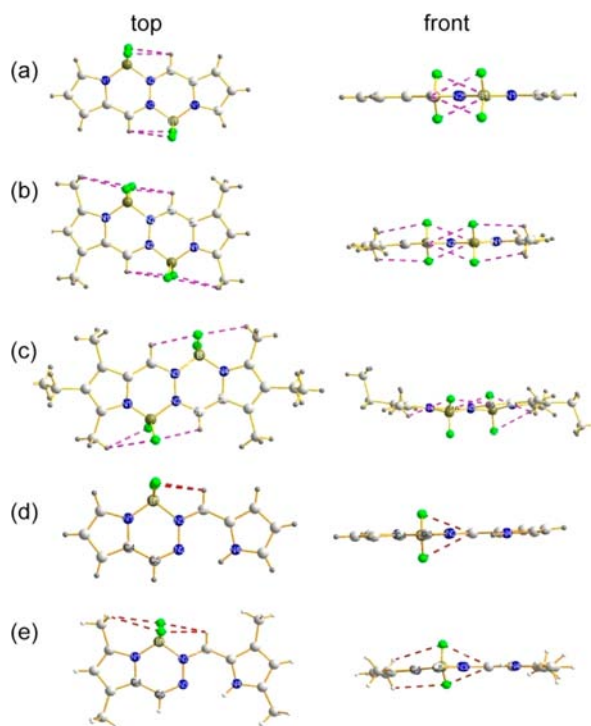


**Figure 2.** X-ray structures of **1a** (a), **1b** (b), **1c** (c), **3a** (d), and **3b** (e). Key: C, light gray; H, gray; N, blue; B, dark yellow; F, bright green.

hydrogen atoms at *C*<sub>m</sub> are significantly lower for the latter (7.94 and 7.01 ppm, respectively).

Complexes **1a–d** exhibit excellent optical properties with a strong absorption and emission (fluorescence quantum yield close to unity) in visible regions in several solvents studied as summarized in Figure 3, Table 1, and Table S2 and Figures S5–S8 in the Supporting Information. A gradual red-shift of the absorption and emission was observed with the installation of alkyl groups on the pyrrolic position of the chromophore. For example, the pyrrolic-unsubstituted complex **1a** gave a strong absorption and fluorescence emission at 423 nm ( $\epsilon = 3.98 \times 10^4 \text{ M}^{-1} \cdot \text{cm}^{-1}$ ) and 468 nm in dichloromethane, respectively, which were red-shifted to 478 nm ( $\epsilon = 5.24 \times 10^4 \text{ M}^{-1} \cdot \text{cm}^{-1}$ ) and 504 nm, respectively, for complex **1c** with alkylation at the pyrrolic position of the chromophore. The absorption and emission maxima of complexes **1a–1d** are only slight solvent dependent with an around 2 ns of fluorescence lifetime, comparable to those of classical BODIPYs. Unlike **1a–d**, a low and solvent-dependent fluorescence ( $\phi = 0.06$  in dichloromethane and  $\phi = 0.45$  in hexane, Table S2, Supporting Information) was observed for complex **1e** similar to those previously reported indole-derived dyes.<sup>12</sup> In comparison with complexes **1a,b**, their monoborate analogues **3a,b** exhibited relative short wavelength absorption with low fluorescence quantum yields.

As expected, the installation of electron-donating substituents (NMe<sub>2</sub>) at the *p*-phenyl position of the chromophore to form **4a,b** via the Knoevenagel condensation leads to a significant red-shift of the absorption and emission maxima (Figure 1 and Table 1). For example, **4a** shows a 90 and 80 nm red-shift in their absorption and fluorescence emission spectra, respectively, with respect to **1b**. A similar red-shift was observed for **4b** with respect to **1c**. Unlike their starting materials **1b,c**, both **4a** and **4b** show strong solvent-dependent fluorescence. As shown in Table S2 and Figures S10 and S11 (Supporting Information), both **4a** and **4b** show large bathochromic shifts and fluorescence quenching in

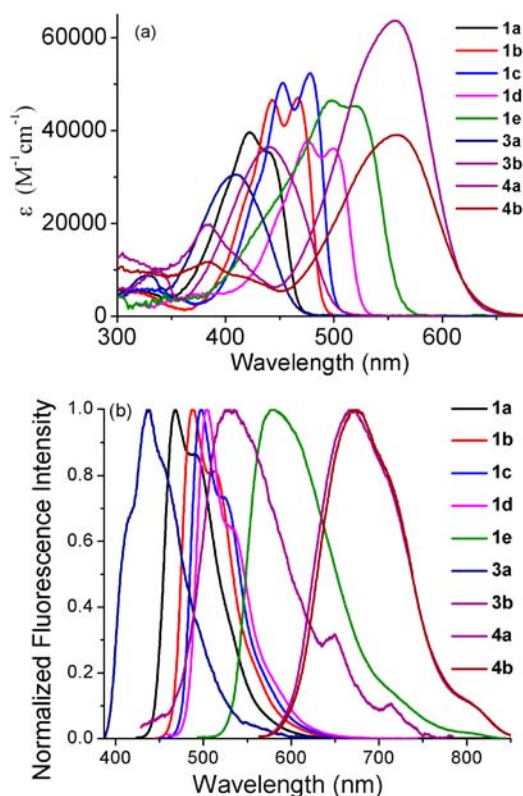


Figure 3. Normalized absorption (a) and fluorescence emission (b) spectra of complexes **1a–e**, **3a,b**, and **4a,b** in dichloromethane.

Table 1. Photophysical Properties of Complexes **1a–e**, **3a,b**, and **4a,b** at Room Temperature in Dichloromethane, Thin Film, and Solid Powder States

	dichloromethane		thin film	solid powder
	$\lambda_{\text{abs}}^{\text{max}}/\text{nm}$ (lg $\epsilon$ )	$\lambda_{\text{em}}^{\text{max}}/\text{nm}$ ( $\tau^a/\text{ns}$ , $\phi^c$ )	$\lambda_{\text{em}}^{\text{max}}/\text{nm}$ ( $\phi^c$ )	$\lambda_{\text{em}}^{\text{max}}/\text{nm}$ ( $\phi^c$ )
<b>1a</b>	423 (4.60), 442 <sup>a</sup>	468 (2.24, 1.00)	537 (0.15)	543 (0.12)
<b>1b</b>	444, <sup>a</sup> 467 (4.67)	487 (2.66, 1.00)	534 (0.12)	550 (0.28)
<b>1c</b>	453, <sup>a</sup> 478 (4.72)	497 (2.66, 1.00)	558 (0.08)	605 (0.19)
<b>1d</b>	455 (4.58), 480 <sup>a</sup>	504 (2.58, 1.00)	575 (0.12)	576 (0.10)
<b>1e</b>	498 (4.67), 522 <sup>a</sup>	580 (1.06, 0.06)	667 (0.04)	673 (0.07)
<b>3a</b>	410 (4.49)	438 (2.13, 0.04)	522 (0.05)	526 (0.06)
<b>3b</b>	441 (4.56)	530 (2.29, 0.03)	585 (0.03)	587 (0.05)
<b>4a</b>	526, <sup>a</sup> 557 (4.80)	667 (1.44, 0.20)	726 (0.02)	754 (0.14)
<b>4b</b>	536, <sup>a</sup> 557 (4.59)	670 (1.61, 0.21)	710 (0.01)	725 (0.11)

<sup>a</sup>Shoulder peak. <sup>b</sup>Fluorescence lifetime. <sup>c</sup>Fluorescence quantum yield; see the Supporting Information for details.

their fluorescence spectra with the increase of the solvent polarity. For example, **4a** emits at 581 nm with fluorescence quantum yield of 0.45 in hexane which was red-shifted to 721 nm with a reduced fluorescence quantum yield of 0.01 in acetonitrile. This indicates the presence of an intramolecular charge transfer (ICT) process<sup>10</sup> in complexes **4a,b**. In addition, complexes **4a,b** are sensitive to the pH variation of the system. The addition of TFA to their dichloromethane solutions induced a blue-shift of absorption from 672 nm to 485 and 512 nm for **4a** and from 667 to 540 nm for **4b** (Figures S12 and S13, Supporting Information) due to the protonation of NMe<sub>2</sub> group.

Most of these complexes also show strong fluorescence emission in the thin film and solid powder states, covering the range of visible to near IR regions (Figure 4 and Figures S14–

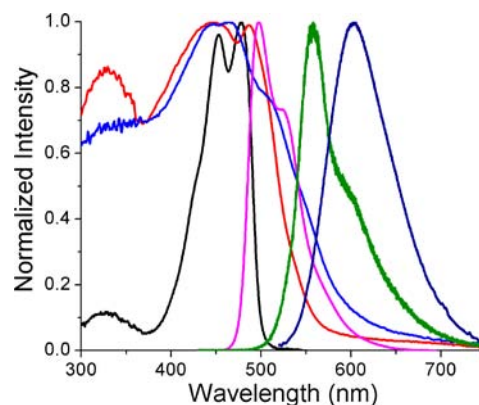


Figure 4. Normalized absorption of **1c** in dichloromethane (black), thin film (red), and powder solid (blue) states and normalized fluorescence emission spectra of **1c** in dichloromethane (magenta), thin film (olive), and powder solid (navy) states.

S22 in the Supporting Information), while BODIPY dyes barely exhibit fluorescence in their solid state.<sup>10a</sup> The broader absorption spectra and fluorescence emission bands in the solid states for all complexes are red-shifted with respect to corresponding absorption and emission bands in solutions. For example, complexes **1b** and **1c** show strong fluorescence at 550 nm ( $\phi = 0.28$ ) and 605 nm ( $\phi = 0.19$ ) in the solid powder state, respectively (Figure 4 and Table 1). More importantly, complexes **4a** and **4b** show relatively strong near-infrared fluorescence at 754 nm ( $\phi = 0.14$ ) and 725 nm ( $\phi = 0.11$ ) in their solid powder state (Figures S21–S22 in the Supporting Information), which are extremely rare for organoboron materials.<sup>13</sup> The high solid state fluorescence of dyes **1a–c** is in agreement with their crystal-packing structures. These dyes all give well ordered packing structures due to multiple intermolecular C–H...F hydrogen bonds (Figures S1–S3 in the Supporting Information). However, no significant  $\pi$ – $\pi$  interactions were observed from crystal packing structures of dyes **1a** and **1b**. Slipped dimers are formed in crystal packing structure of **1c** (Figures S3) which are typical J-aggregates.<sup>6a</sup>

The cyclic voltammetry of complexes **1a–c** were performed in deoxygenated dichloromethane at room temperature containing tetrabutylammonium hexafluorophosphate (TBAPF<sub>6</sub>) as the supportive electrolyte. As shown in Figure 5, complexes **1a**, **1b**, and **1c** display an irreversible reduction wave with  $E_{\text{pc}}$  at  $-1.14$ ,

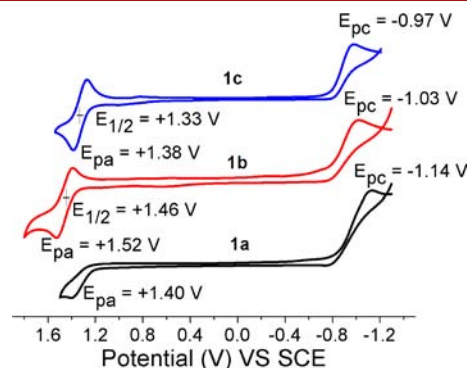


Figure 5. Cyclic voltammograms of 1 mM **1a–c** measured in dichloromethane solution, containing 0.1 M TBAPF<sub>6</sub> as the supporting electrolyte at room temperature. Glassy carbon electrode as a working electrode, and the scan rate at 50 mV s<sup>-1</sup>.



−1.03, and −0.97 V. One irreversible oxidation wave for **1a** and reversible oxidation waves for **1b** and **1c** were observed with  $E_{pa}$  at 1.40 V (**1a**) and half-wave potentials at 1.46 and 1.33 V (vs SCE) (**1b** and **1c**), respectively. HOMO energy levels of −5.80, −5.74, and −5.56 eV and LUMO energy levels of −3.57, −3.80, and −3.66 eV were estimated for complexes **1a–c**, respectively, based on their onset potential of the first oxidation and reduction waves. Thus, the installation of alkyl groups on the pyrrolic position indeed helps the decrease the LUMO level of the chromophore and the decrease of the energy band gaps. Electrochemical energy band gaps for complexes **1a–c** were calculated to be 2.23, 1.94, and 1.90 eV, respectively, which is in well correlation with their optical band gaps.

To test their potential practical applications as novel dyes, we also studied the photostabilities of these resultant complexes in toluene under continuous irradiation with a 500 W Xe lamp (Figure S23, Supporting Information). As demonstrated by complexes **1a** and **1d** in Figure S23a (Supporting Information), both complexes show excellent photostabilities during the period of strong irradiation (60 min): more than 98% amount of **1a** and **1d** remained, while only 76% of the well-known commercialized 1,3,5,7-tetramethylBODIPY (4,4-difluoro-1,3,5,7-tetramethyl-4-bora-3a,4a-diaza-s-indocene) left under the same condition. In addition, these dyes are also stable in aqueous solution as shown in Figure S23c (Supporting Information). The photostability of **1a** in aqueous DMSO solution is much better than that of fluorescein in 0.1 M NaOH solution.

In summary, we have developed an efficient synthesis of a series of  $\text{BF}_2$  complexes of hydrazine–Schiff base linked bispyrrole via a simple two-step reaction from commercially available substances. These resultant complexes are highly fluorescent in solution, film, and solid states with excellent photostabilities over the well-known commercialized 1,3,5,7-tetramethylBODIPY. The photophysical properties of these novel dyes are easily tunable through the structural variation of the starting 2-formylpyrrole and thereof their analogues like 2-formylindole demonstrated in this work and through the facile postfunctionalizations from the Knoevenagel condensation reaction as demonstrated here. The efficient synthetic methodology presented here may find applications in the facile access of a variety of boron-containing organic fluorescent dyes.

## ■ ASSOCIATED CONTENT

### Supporting Information

Experimental details, NMR, additional photophysical data, and CIF. This material is available free of charge via the Internet at <http://pubs.acs.org>.

## ■ AUTHOR INFORMATION

### Corresponding Authors

\*E-mail: [jiao421@mail.ahnu.edu.cn](mailto:jiao421@mail.ahnu.edu.cn).

\*E-mail: [haoehong@mail.ahnu.edu.cn](mailto:haoehong@mail.ahnu.edu.cn).

### Notes

The authors declare no competing financial interest.

## ■ ACKNOWLEDGMENTS

This work is supported by the National Nature Science Foundation of China (Grants Nos. 21072005, 21272007 and 21372011) and the Research Culture Funds of Anhui Normal University (Grant No. 160-791310).

## ■ REFERENCES

- (1) (a) Vendrell, M.; Zhai, D.; Er, J. C.; Chang, Y.-T. *Chem. Rev.* **2012**, *112*, 4391. (b) Kobayashi, H.; Ogawa, M.; Alford, R.; Choyke, P. L.; Urano, Y. *Chem. Rev.* **2010**, *110*, 2620. (c) Yuan, L.; Lin, W.; Zheng, K.; He, L.; Huang, W. *Chem. Soc. Rev.* **2013**, *42*, 622.
- (2) (a) Loudet, A.; Burgess, K. *Chem. Rev.* **2007**, *107*, 4891. (b) Ulrich, G.; Ziesler, R.; Harriman, A. *Angew. Chem., Int. Ed.* **2008**, *47*, 1184. (c) Boens, N.; Leen, V.; Dehaen, W. *Chem. Soc. Rev.* **2012**, *41*, 1130. (d) Awuah, A. G.; You, Y. *RSC Adv.* **2012**, *2*, 11169. (e) Lu, H.; Mack, J.; Yang, Y.; Shen, Z. *Chem. Soc. Rev.* **2014**, DOI: 10.1039/c4cs00030g.
- (3) (a) Heyer, E.; Retailleau, P.; Ziesler, R. *Org. Lett.* **2014**, *16*, 2230. (b) Kolen, S.; Cakmak, Y.; Kostereli, Z.; Akkaya, E. U. *Org. Lett.* **2014**, *16*, 660. (c) Manjare, S. T.; Kim, J.; Lee, Y.; Churchill, D. G. *Org. Lett.* **2014**, *16*, 520. (d) Leen, V.; Yuan, P.; Wang, L.; Bones, N.; Dehaen, W. *Org. Lett.* **2012**, *14*, 6150. (e) Jiang, T.; Zhang, P.; Yu, C.; Yin, J.; Jiao, L.; Dai, E.; Wang, J.; Wei, Y.; Mu, X.; Hao, E. *Org. Lett.* **2014**, *16*, 1952.
- (4) (a) Frath, G.; Massue, J.; Ulrich, G.; Ziesler, R. *Angew. Chem., Int. Ed.* **2014**, *53*, 2290. (b) Zhao, D.; Li, G.; Wu, D.; Qin, X.; Neuhaus, P.; Cheng, Y.; Yang, C.; Lu, Z.; Pu, X.; Long, C.; You, J. *Angew. Chem., Int. Ed.* **2013**, *52*, 13676. (c) Aranedra, J.; Piers, W. E.; Heyne, B.; Parvez, M.; McDonald, R. *Angew. Chem., Int. Ed.* **2011**, *50*, 12214. (d) Saito, S.; Matsuo, K.; Yamaguchi, S. *J. Am. Chem. Soc.* **2012**, *134*, 9130. (e) Glotzbach, C.; Kauscher, U.; Voskuhl, J.; Kehr, N. S.; Stuart, M. C. A.; Fröhlich, R.; Galla, H. J.; Ravoo, B. J.; Nagura, K.; Saito, S.; Yamaguchi, S.; Würthwein, E. U. *J. Org. Chem.* **2013**, *78*, 4410.
- (5) (a) Frath, D.; Azizi, S.; Ulrich, G.; Retailleau, P.; Ziesler, R. *Org. Lett.* **2011**, *13*, 3414. (b) Frath, D.; Azizi, S.; Ulrich, G.; Ziesler, R. *Org. Lett.* **2012**, *14*, 4774. (c) Benelhadj, K.; Massue, J.; Retailleau, P.; Ulrich, G.; Ziesler, R. *Org. Lett.* **2013**, *15*, 2918.
- (6) (a) Kubota, Y.; Tsuzuki, T.; Funabiki, K.; Ebihara, M.; Matsui, M. *Org. Lett.* **2010**, *12*, 4010. (b) Kubota, Y.; Hara, H.; Tanaka, S.; Funabiki, K.; Matsui, M. *Org. Lett.* **2011**, *13*, 6544. (c) Kubota, Y.; Tanaka, S.; Funabiki, K.; Matsui, M. *Org. Lett.* **2012**, *14*, 4682. (d) Kubota, Y.; Ozaki, Y.; Funabiki, K.; Matsui, M. *J. Org. Chem.* **2013**, *78*, 7058.
- (7) (a) Wu, Y.; Chen, Y.; Gou, G.; Mu, W.; Lv, X.; Du, M.; Fe, W. *Org. Lett.* **2012**, *14*, 5226. (b) Li, W.; Lin, W.; Wang, J.; Guan, X. *Org. Lett.* **2013**, *15*, 1768. (c) Curiel, D.; Ms-Montoya, M.; Usea, L.; Espinosa, A.; Orenes, R. A.; Molina, P. *Org. Lett.* **2012**, *14*, 3360.
- (8) (a) Suresh, D.; Gomes, C. S. B.; Gomes, P. T.; Di Paola, R. E.; Macanita, A. L.; Calhorda, M. J.; Charas, A.; Morgado, J.; Duarte, M. T. *Dalton Trans.* **2012**, *41*, 8502. (b) Yang, Y.; Hughes, R. P.; Aprahamian, J. *J. Am. Chem. Soc.* **2012**, *134*, 15221. (c) Li, H.; Fu, W.; Gan, X.; Mu, W.; Chen, W.; Duan, X.; Song, H. *Org. Lett.* **2010**, *12*, 2924. (d) Fischer, G. M.; Daltrozzi, E.; Zumbush, A. *Angew. Chem., Int. Ed.* **2011**, *50*, 1406.
- (9) Tamgho, I.-S.; Hasheminasab, A.; Engle, J. T.; Nemykin, V. N.; Ziegler, C. J. *J. Am. Chem. Soc.* **2014**, *136*, 5623.
- (10) (a) Rurack, K.; Kollmannberger, M.; Daub, J. *Angew. Chem., Int. Ed.* **2001**, *40*, 385. (b) Coskun, A.; Akkaya, E. U. *J. Am. Chem. Soc.* **2005**, *127*, 10464. (c) Ozlem, S.; Akkaya, E. U. *J. Am. Chem. Soc.* **2009**, *131*, 48. (d) Buyukcakar, O.; Bozdemir, O. A.; Kolen, S.; Erbas, S.; Akkaya, E. U. *Org. Lett.* **2009**, *11*, 4644. (e) Bura, T.; Retailleau, P.; Ulrich, G.; Ziesler, R. *J. Org. Chem.* **2011**, *76*, 1109.
- (11) (a) Zhang, M.; Hao, E.; Xu, Y.; Zhang, S.; Zhu, H.; Wang, Q.; Yu, C.; Jiao, L. *RSC Adv.* **2012**, *2*, 11215. (b) Wu, L.; Burgess, K. *Chem. Commun.* **2008**, 4933.
- (12) (a) Wakamiya, A.; Murakami, T.; Yamaguchi, S. *Chem. Sci.* **2013**, *4*, 1002. (b) Ni, Y.; Zeng, W.; Huang, K.; Wu, J. *Chem. Commun.* **2013**, *49*, 1217. (c) Shimogawa, H.; Mori, H.; Wakamiya, A.; Murata, Y. *Chem. Lett.* **2013**, *42*, 986. (d) Yu, C.; Xu, Y.; Jiao, L.; Zhou, J.; Wang, Z.; Hao, E. *Chem.—Eur. J.* **2012**, *18*, 6437.
- (13) Cheng, X.; Li, D.; Zhang, Z.; Zhang, H.; Wang, Y. *Org. Lett.* **2014**, *16*, 880.